ORIGINAL RESEARCH

Homogenous hydrolysis of cellulose to glucose in an inorganic ionic liquid catalyzed by zeolites

Tao Wu · Ning Li · Xuejun Pan · Sheng-Li Chen

Abstract Zeolites (ZSM-5 and Beta) with different SiO_2/Al_2O_3 ratios were synthesized as solid acids for hydrolyzing cellulose in an inorganic ionic liquid system (lithium bromide trihydrate solution, LBTH) under mild conditions. The results indicated that the texture properties of zeolite had little effect on catalytic activity, while acidity of zeolite was crucial to the cellulose hydrolysis. In the LBTH system, H-form zeolites released H^+ into the solution from their acid sites via ion-exchange with $Li^+$, which hydrolyzed the cellulose already dissolved. This unique homogeneous hydrolysis mechanism was the primary reason for the excellent performance of the zeolites in catalyzing cellulose hydrolysis in the LBTH system. It was found cellulose could be completely hydrolyzed to glucose and oligoglucan by 2% (w/w on cellulose) zeolite at 140 °C within 3 h with a single-pass glucose yield 61%. The zeolites could be recovered with 50% initial catalytic activity after regeneration and reused with stable catalytic activity.

T. Wu · N. Li · X. Pan (✉)
Department of Biological Systems Engineering,
University of Wisconsin-Madison, 460 Henry Mall,
Madison, WI 53706, USA
e-mail: xpan@wisc.edu

T. Wu · S.-L. Chen
State Key Laboratory of Heavy Oil Processing, College of Chemical Engineering, China University of Petroleum-Beijing, Beijing 102249, People's Republic of China

Graphic abstract
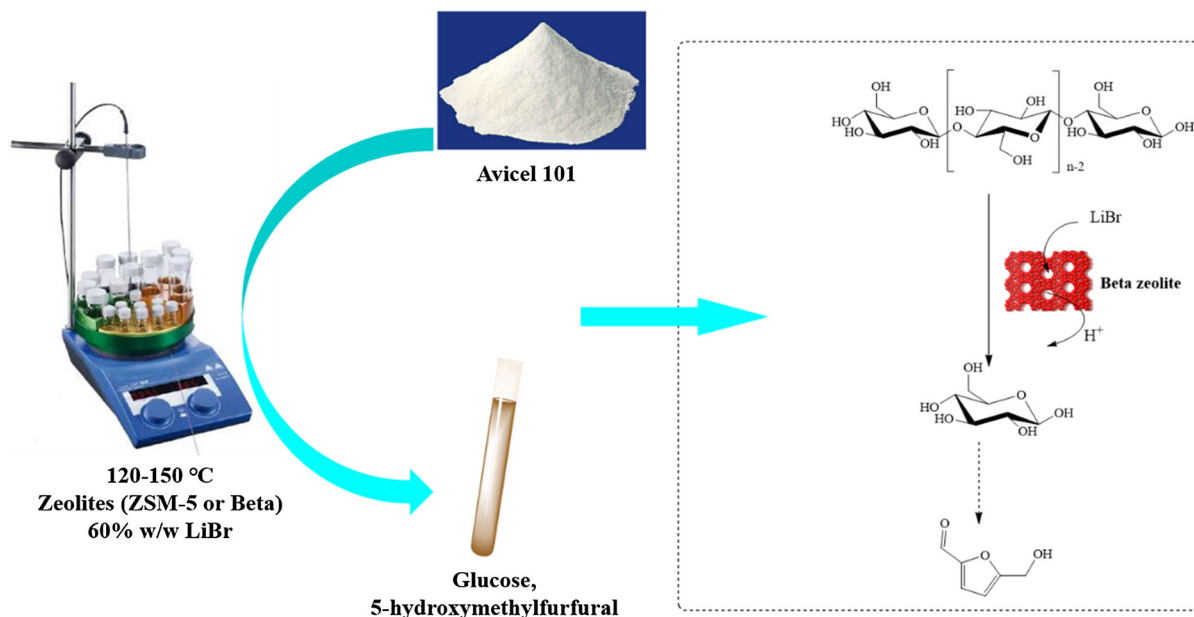
Introduction

As the most abundant natural polymer, cellulose has been consensually considered as a renewable resource to replace fossil for sustainable production of chemicals and fuels (Huang et al. 2019). Effective hydrolysis of cellulose to glucose is a key step for the conversion of lignocellulosic biomass to liquid fuels and value-added chemicals via so-called sugar platform (Jiang et al. 2019; Mu et al. 2019).

Mineral acids, such as H_2SO_4 and HCl, are the most common catalysts for hydrolyzing cellulose to glucose (Rinaldi and Schuth 2010). Although they are effective, the mineral acids have issues related to equipment erosion, poor selectivity, and acid recovery. Enzyme (cellulase) is a selective catalyst which works effectively at moderate temperature (Hammerer et al. 2018). However, the cellulase suffers from high price, slow reaction, and poor reusability. Solid acids have attracted more attention in recent years for cellulose hydrolysis (Huang and Fu 2013; Shrotri et al. 2018),

because of their easy separation, good recyclability, and competitive price. Among the solid acids investigated, zeolite has been proven to be a unique catalyst for cellulose hydrolysis owing to its tunable acidity and special shape selectivity (Chu et al. 2018). Onda et al. (2008) found that the H-Beta and H-ZSM-5 zeolites with high Si/Al ratio could catalyze cellulose hydrolysis to glucose with a yield of 12%. Other zeolites (H-USY, H-MOR, SAPO-34, Al-MCM-41 and Al-SBA-15) have also been employed in cellulose hydrolysis in recent decade (Jiang et al. 2014; Zhou et al. 2013).

However, zeolites are usually not as effective as homogeneous mineral acids and enzymes in catalyzing cellulose hydrolysis in water because of the limited interaction between the solid zeolite and solid cellulose. To improve the hydrolysis efficiency, one strategy is to dissolve cellulose in a solvent such as ionic liquid and then hydrolyze it with zeolites. For example, Cellulose dissolved in [C4mim]Cl was hydrolyzed by HY zeolite with SiO_2/Al_2O_3 molar ratio of 5, yielding 36.9% glucose (Zhang and Zhao 2009). Another study (Cai et al. 2012) reported a glucose yield of 50.0% using HY zeolite on dissolved cellulose in [Bmim]Cl. One of the issues in zeolite-catalyzed cellulose hydrolyses is the high loading of the catalyst. For example, it was reported that a

desilicated ZSM-5 zeolite was able to hydrolyze cellulose by 63.9%, but the mass ratio of zeolite to cellulose was as high as 1.6 (Chu et al. 2018). In another study (Chen et al. 2018), mass ratio of mesoporous ZSM-5 to cellulose was 1 to reach a 49.6% yield of total reducing sugars.

Some inorganic molten salt hydrates (for example, lithium bromide trihydrate (LBTH), LiBr·3H$_2$O) were found to be capable of dissolving cellulose and thereby facilitate acidic cellulose hydrolysis under moderate conditions (low temperature and acid concentration) (Deng et al. 2015; Yang et al. 2016). Pan et al. (Li et al. 2016, 2018a) explored cellulose and biomass saccharification in acidic lithium bromide trihydrate (ALBTH) system using homogeneous acid (such as hydrochloric and sulfuric acid) as a catalyst. It was found that cellulose and hemicelluloses in the biomass could be quickly and completely dissolved and hydrolyzed under mild conditions, and meanwhile lignin was depolymerized in solid state without condensation. Another unique property of the molten salt hydrate is that it enhances acidity of an acid. In other words, the acidity of an acid is significantly higher in a molten salt hydrate than in water at the same acid concentration (Franzyshen et al. 1990), which allows to lower the acid loading as catalyst and thereby reduce the acid-induced sugar degradation during cellulose hydrolysis.

Considering the issues (high viscosity of solvent, high loading of catalyst, and unsatisfactory yield of cellulose hydrolysis to glucose) of the reported organic ionic liquid-zeolite systems for cellulose hydrolysis and the unique properties (such as low viscosity and enhanced acidity) of inorganic molten salt hydrate (inorganic ionic liquid) system, we hypothesized that (1) zeolite could efficiently hydrolyze cellulose dissolved in the LBTH system; (2) the enhanced acidity in the LBTH would allow to significantly reduce zeolite loading; and (3) tuning zeolite structure would be able to further improve the performance of zeolite-catalyzed cellulose hydrolysis in the LBTH. Therefore, in this study, we investigated the cellulose hydrolysis catalyzed by zeolites in the LBTH system to test the hypotheses. ZSM-5 zeolite and Beta zeolite were synthesized and characterized, and then used for catalyzing cellulose hydrolysis in the LBTH system under different conditions. The catalytic behaviors of the zeolites were investigated, and the effects of zeolite's properties (surface areas, pore size, and distribution of acid sites) on the cellulose hydrolysis were studied.

Materials and methods

Chemicals and materials

Template, tetrapropylammonium bromide (TPABr, 98%), was purchased from Tokyo chemical industry Co., LTD. Lithium bromide (99%) and microcrystalline cellulose (Avicel PH101, 50 μm) were purchased from Sigma Aldrich (St Louis, MO). Lithium bromide (LiBr) was obtained from Alfa Aesar (Haverhil, MA). Aqueous LiBr solution (e.g., 60 wt%) was prepared by dissolving LiBr in water. Sodium aluminum oxide (NaAlO$_2$, 99%), silica gel (150–230 mesh), ammonium nitrate (95%), and tetraethylammonium hydroxide (TEAOH, 35%) were purchased from Alfa Aesar (Tewksbury, MA). Sodium hydroxide (NaOH, 50%) was purchased from VWR (Radnor, PA). All the chemicals were used as received without further purification.

Synthesis of zeolites

H-form ZSM-5 zeolite with SiO$_2$/Al$_2$O$_3$ molar ratio of x (x = 30 or 50, molar ratio in the reagent mixture) and H-form Beta zeolite with SiO$_2$/Al$_2$O$_3$ molar ratio of y (y = 30 or 50, molar ratio in the reagent mixture) were synthesized hydrothermally by using TPABr and TEAOH as template, respectively (Wu et al. 2017, 2018). NaAlO$_2$, silica gel, and NaOH were used as aluminum, silicon, and alkali source, respectively. A typical synthesis procedure of ZSM-5 is described in supporting information. The obtained H-form ZSM-5 and Beta zeolites were labeled as Z-5-x and Beta-y, respectively.

Hydrolysis of cellulose with zeolites

In brief, a certain amount of zeolite, 500 mg of Avicel, and 5.00 mL 60% w/w LiBr solution were mixed in a Teflon vial (Saville, USA). The hydrolysis experiments were conducted at a preset temperature (T: 120–150 °C in an oil bath) with a magnetic stirrer (600 rpm) for a certain time. After the hydrolysis reaction, the mixture was filtrated. 5-Hydroxymethylfurfural (HMF) and glucose in the filtrate was

quantified by high performance liquid chromatography (HPLC) and high-performance ion chromatography (HPIC), respectively, as described below. All hydrolysis experiments were carried out in duplicates, and average result was reported.

Post-hydrolysis

Quantitation of the total oligosaccharides in the hydrolysate was conducted following a post-hydrolysis procedure that converted all the oligosaccharides to glucose before HPIC analysis. Briefly, the hydrolysate (including residual glucose and oligosaccharides) from the hydrolysis reaction was hydrolyzed in 4% sulfuric acid at 121 °C for 1 h in an autoclave unit to convert oligosaccharides to glucose. After neutralization, glucose in the post-hydrolysate was quantitated using the HPIC method. The free glucose in the hydrolysate before the post-hydrolysis was quantitated using the same HPIC method. The difference gave the yield of the oligosaccharides (Y), calculated by following Eq. 1.

$$Y = \frac{M_{\text{Glucose}} - M_{\text{Gulcose},t}}{M_{\text{Cellulose},0} \times \frac{180}{162}} \times 100\% \qquad (1)$$

where M_{Glucose} is the total mass of glucose after post hydrolysis, and $M_{\text{Glucose},t}$ is the mass of glucose after cellulose hydrolysis before the post hydrolysis. $M_{\text{Cellulose},0}$ is the mass of starting cellulose.

Recycling of zeolites

After completion of a cellulose hydrolysis reaction, the catalyst zeolite was collected by vacuum filtration and thoroughly washed with water. Then, the used zeolite was dried and then calcined at 550 °C for 3 h to measure the mass loss of zeolite samples during the reaction before regeneration. The catalyst was regenerated by ion exchange with 1 M NH_4NO_3 solution and calcination according to the procedure of synthesis described in supporting information.

Characterization and analysis

X-ray diffraction (XRD) analysis was conducted on a Bruker D8 Advance instrument, using Cu Kα radiation ($\lambda = 1.54$ Å) as X-ray source and operated at 40 kV and 30 mA. The scanning range of 2θ was 5°–50°.

Scanning electron microscope (SEM) images were collected on a FEI Quanta 200F high-resolution SEM at an operating voltage of 2000 kV.

N_2 adsorption–desorption experiment of the zeolite samples was conducted on a Micrommeritics ASAP 2020 instrument. Before the experiment, all samples were pretreated at 250 °C under vacuum of 10^{-3} Pa for 15 h. The adsorption–desorption was conducted at -196 °C.

The type and concentration of acid sites were identified and determined by the adsorption of pyridine, and the Fourier Transform Infrared (Py-FTIR) spectra were recorded on a Bruker IFS 66 spectrometer. Prior to the measurement, the sample was pretreated under 10^{-4} kPa and 400 °C for 3 h. The sample was then baked at 150 °C for 1 h to remove the weakly absorbed and gaseous molecules before FTIR spectra were recorded at this temperature. Three absorption peaks, correlating to the Brønsted and Lewis acid sites of zeolite, are appeared in the range of 1400–1700 cm^{-1} on all the spectra. The peak close to 1540 cm^{-1} was related to Brønsted acid sites; the peak near 1450 cm^{-1} was ascribed to Lewis acid sites; and the peak near 1490 cm^{-1} was corresponding to the combination of Brønsted and Lewis acid sites (Woolery et al. 1997). According to the methods reported by Madeira and co-workers (Ferreira Madeira et al. 2012), the concentrations of Brønsted and Lewis acid sites can be calculated as following.

$$C_{\text{B/L}} = \frac{A}{\varepsilon} \times \frac{S}{m} \qquad (2)$$

where $C_{\text{B/L}}$ is the concentration of Brønsted or Lewis acid sites (mmol g^{-1}), S is the surface area of the sample wafer, A is the integrated area of the peak at 1450 or 1540 cm^{-1}, ε is the molar extinction coefficient (Lewis and Brønsted acid sites were 1.28 cm μmol^{-1} and 1.13 cm μmol^{-1}, respectively), and m is the mass of zeolite sample (mg).

Temperature-programmed desorption of ammonia (NH_3-TPD) was performed on a self-built adsorption instrument. Prior to the adsorption, zeolite sample (100 mg) was pretreated at 600 °C for 1 h and then cooled to 110 °C under N_2 atmosphere. Subsequently, to reach a saturated adsorption state, the sample was treated with anhydrous NH_3 stream for 0.5 h at 110 °C, followed by flushing with N_2 for 1 h at 110 °C to remove gaseous and weak adsorbed NH_3. Finally, the sample was heated linearly from 110 to

600 °C with a heating rate of 10 °C min^{-1}, and the desorption of the NH$_3$ was detected by a thermal conductivity detector (TCD).

To determine the conversion of cellulose (x), the residual cellulose after the hydrolysis was collected by filtration, dried at 110 °C in an oven for 24 h, and quantitated gravimetrically (we assumed that zeolite mass did not change during the hydrolysis). Glucose was quantified using a HPIC system (ICS-3000, Dionex, Sunnyvale, CA) equipped with integrated amperometric detector and Carbopac^{TM} PA1 guard and analytic columns, as described earlier (Shuai et al. 2010). HMF was analyzed using a HPLC system (ICS-3000, Dionex, Sunnyvale, CA) equipped with a Supelcogel C-610H column (7.8 × 300 mm) at 30 °C and an UV detector at 210 nm. An isocratic flow of deionized water containing 0.1% phosphoric acid was used as the mobile phase at 0.6 mL min^{-1} (Shuai et al. 2010). Yields of glucose and HMF were calculated as a weight percentage of theoretically available ones in the starting cellulose. Conversion (x) of cellulose, glucose yield (y), and HMF yield (z) were defined by Eqs. 3–5, respectively.

$$x = \left(1 - \frac{M_{\text{Cellulose},t}}{M_{\text{Cellulose},0}}\right) \times 100\% \quad (3)$$

$$y = \frac{M_{\text{Glucose},t}}{M_{\text{Cellulose},0} \times \frac{180}{162}} \times 100\% \quad (4)$$

$$z = \frac{M_{\text{HMF},t}}{M_{\text{Cellulose},0} \times \frac{126}{162}} \times 100\% \quad (5)$$

where $M_{\text{Cellulose},0}$ and $M_{\text{Cellulose},t}$ are the mass of starting cellulose before hydrolysis and the residual cellulose after hydrolysis, respectively. $M_{\text{Glucose},t}$ and $M_{\text{HMF},t}$ represent the mass of glucose and HMF at time t, respectively.

Results and discussion

Characteristics of zeolites

As shown in Fig. 1, zeolite ZSM-5 and Beta had typical MFI (JCPDS No. 42-0024) and BEA (JCPDS No. 47-0183) topology with a negligible impurity phase and high crystallinity, respectively. Amorphous silica-alumina (impurity phase), usually having weak acidity and small surface area, is seldom used in acid
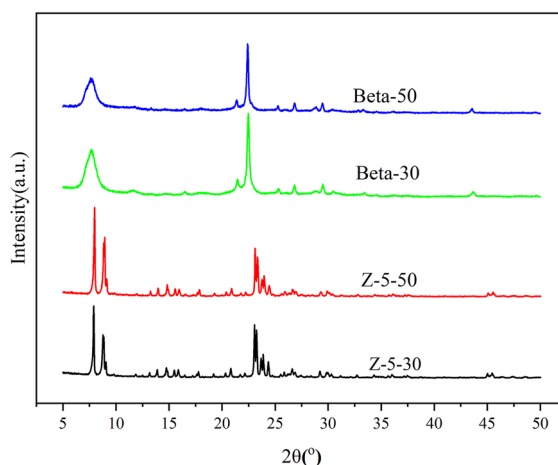

Fig. 1 XRD patterns of zeolites

catalyzed reactions. The relative crystallinity and crystal size of the zeolites were calculated and presented in Table S1 (in Electronic Supplementary Material: ESM). Z-5-30 and Z-5-50 had similar crystal size, ascribed to the same synthesis process, so did Beta-30 and Beta-50. Crystal size of Beta was much smaller than that of ZSM-5.

The morphologies of ZSM-5 series and Beta series were studied using SEM, and the images are depicted in Fig. S1 (in ESM). ZSM-5 had short columnar shape, while Beta zeolite appeared in irregular spherical shape with particle size ranging from 200 to 600 nm. It is known that morphology and crystal size of zeolites have a great effect on zeolite's physical properties and distribution of acid sites, which further influence the catalytic performance in most zeolite catalyzed reactions (Guo et al. 2019; Xiang and Wu 2019).

The textural properties of the zeolites are summarized in Table 1. N$_2$ physisorption isotherms and the pore size distribution of the zeolites are shown in Fig. S2 (in ESM). It was observed that ZSM-5 series possessed a uniform mesoporous structure, while Beta zeolites did not. Beta zeolites had higher BET surface but lower external surface than ZSM-5 zeolites due to their different pore structure, crystal size, and morphology. ZSM-5 series with different SiO$_2$/Al$_2$O$_3$ ratios (Z-5-30 and Z-5-50) had nearly the same surface and pore structure, ascribed to the same synthesis process, so did Beta-30 and Beta-50. Due to its large molecular size, cellulose is unable to enter the crystal pore (micropore) of zeolite. Therefore, in a heterogenous catalytic system like the zeolite-catalyzed

Table 1 Textural properties of zeolites

Zeolite	Surface area (m² g⁻¹)			Volume (m³ g⁻¹)	
	S_{BET}^a	S_{Exter}^b	S_{Micro}^c	V_{Micro}^d	V_{Meso}
Z-5-30	481	158	323	0.14	0.27
Z-5-50	454	126	328	0.16	0.24
Beta-30	531	65	466	0.32	0.10
Beta-50	523	61	462	0.30	0.11

[a]BET surface area

[b]t-plot external surface area

[c]t-plot micropore surface area

[d]t-plot micropore volume

cellulose hydrolysis, large mesopore volume may benefit the contact/interaction between reactant (cellulose) and acid sites located at zeolite framework, and thereby ensure high cellulose hydrolysis.

Since the acidic properties (type, concentration and strength of acid sites) of the zeolites are vital factors for zeolite catalyzed reactions, the zeolites were studied using Py-FTIR to identify and quantitate their acid sites. The Py-FTIR spectra are depicted in Fig. 2 and the acid type and concentration are listed in Table 1. In general, a zeolite with higher Si/Al ratio possessed lower acid concentration due to lower content of alumina that services as the acid site. Z-5-30 and Beta-30 with the same Si/Al ratio had similar acid concentration, so did Z-5-50 and Beta-50. It was

reported that in zeolite catalyzed cellulose hydrolysis, Brønsted acid sites provide/release proton serving as active centers for cellulose hydrolysis (Li et al. 2018b), while Lewis acid sites promote glucose degradation (Marianou et al. 2018; Swift et al. 2016). As shown in Table 1, two series of zeolites synthesized in this study both possessed low content of Lewis acid sites, which should be one of the reasons why the zeolites gave lower HMF yield, as discussed below.

Unlike homogeneous acids (HCl and H_2SO_4), a solid acid does not have a unique acid strength. The acid strength of each acid site is determined by the surrounding chemical environment of aluminum (Etim et al. 2019). NH_3-TPD was conducted to investigate the distribution of acid strength of different zeolites (Fig. 3). Two peaks of ammonia desorption between 110 °C and 600 °C appeared for all samples, suggesting a wide distribution of acid strength. The peak appearing in high temperature range represents strong acid site, and that in low temperature range the weak acid site. The spectra were deconvolved to two Gaussian curves to quantitatively analyze the amount of these two types of acid sites, and the results are shown in Table 2. It is apparent that Z-5-30 had more strong acid sites than Beta-30, so did Z-5-50 than Beta-50. Beta-50 had lower acid concentration but larger proportion of strong acid sites than Beta-30.
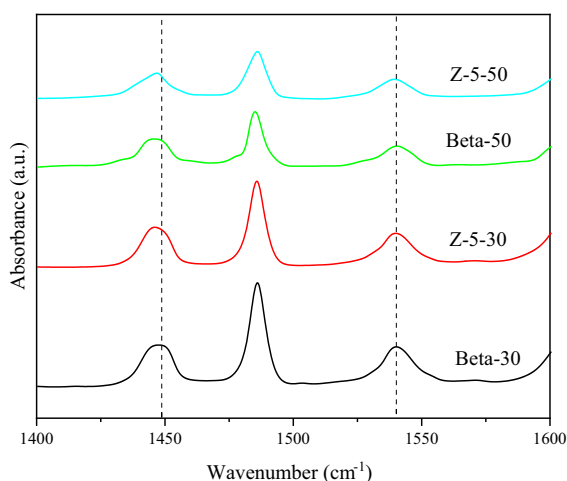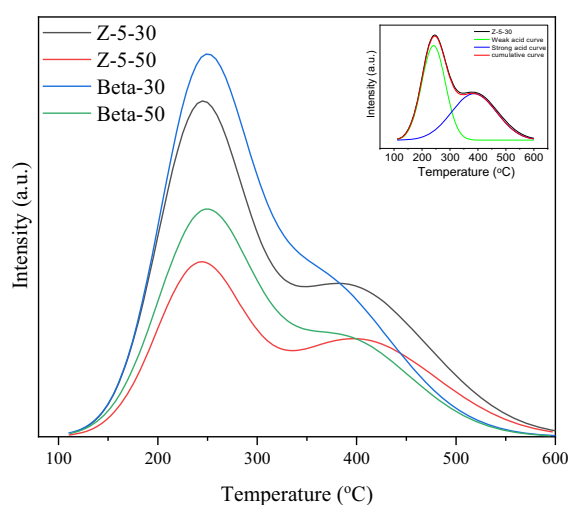

Fig. 2 Py-IR spectra of zeolites (desorption temperature:150 °C)

Fig. 3 NH_3-TPD patterns of zeolites

Table 2 Acidic properties of zeolites

Zeolite	C_B^a	C_L^b	C_S^c	C_W^d	C_T^e	H/L^f
Z-5-30	0.20	0.05	0.14	0.12	0.26	1.2
Z-5-50	0.12	0.03	0.09	0.06	0.15	1.5
Beta-30	0.19	0.05	0.09	0.14	0.23	0.6
Beta-50	0.11	0.03	0.07	0.07	0.14	1.0

[a]Brønsted acid concentration

[b]Lewis acid concentration

[c]Strong acid concentration

[d]Weak acid concentration

[e]Total acid concentration

[f]H/L is the ratio of strong acid concentration to weak acid concentration

Cellulose hydrolysis catalyzed by the zeolites

The catalytic performance of the synthesized zeolites in hydrolyzing cellulose in the LBTH system was evaluated, and it was found that the predominant products from cellulose hydrolysis were glucose and water-soluble oligosaccharides (such as cellobiose) with small amount of HMF from glucose dehydration. For comparison, cellulose hydrolysis was also conducted in pure water (no LiBr) with zeolite (Beta-30) as catalyst and in the LBTH without zeolite, but both cellulose conversion and glucose yield of these two experiments were very low under the same conditions (temperature and time) (Table S2 in ESM).

(1) Effect of reaction time

The time profile of zeolite-catalyzed cellulose hydrolysis (0–8 h) was investigated, and the results are shown in Fig. 4. It seems that the primary hydrolysis of cellulose to oligosaccharides readily occurred in this catalytic system, evidenced by the almost complete conversion of cellulose in short time. However, the secondary hydrolysis of soluble oligosaccharides to glucose was significantly slower than the primary hydrolysis. Therefore, longer time was necessary to reach higher glucose yield. For example, it took 8 h to get a glucose yield of approximately 60% by both Z-5-30 and Beta-30. However, when the reaction time was too long ($\geq$ 7 h), the glucose dehydration was promoted, leading to the formation of HMF, as shown in Fig. 4. Interestingly, Z-5-30 and Beta-30 had different
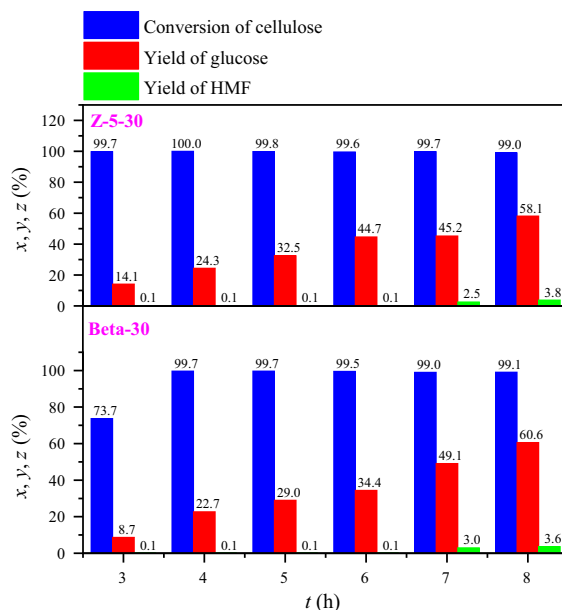

Fig. 4 Hydrolysis of cellulose (Avicel) with zeolites, Z-5-30 and Beta-30. Hydrolysis condition: zeolites (2%, 0.01 g), Avicel (0.5 g), 60% w/w LiBr (5 mL), and 130 °C. t—hydrolysis time (h); x—cellulose conversion (%); y—glucose yield (%); z—HMF yield (%)

textural properties and acid strength but showed comparable catalytic performance in cellulose hydrolysis at the same acid concentration.

(2) Effect of temperature

Generally, elevating temperature is an efficient way to accelerate a reaction. The effect of reaction temperature (120–150 °C) on the cellulose hydrolysis catalyzed by zeolites is shown in Table 3. It was observed that glucose yield increased first and then declined as temperature raised, apparently because high temperature promoted the dehydration of glucose to HMF, which was supported by the increased HMF yield at high temperature. The yield of oligosaccharides was high at lower temperature and decreased monotonically as temperature raised, suggesting that the primary hydrolysis of cellulose to oligosaccharides occurred readily in the LBTH system even at lower temperature. The secondary hydrolysis from oligosaccharides to glucose was slow and the rate-limiting step in the hydrolysis course from cellulose to glucose.

A simplified reaction model proposed by Saeman (1945) divided the cellulose hydrolysis process into

Table 3 Hydrolysis of cellulose catalyzed by zeolites

Entry	T (°C)	L (%)	t (h)	x (%)	y (%)	z (%)	Y (%)
1	120	10	0.5	98.1	28.3	0.2	54.4
2	130	10	0.5	96.4	55.7	1.4	38.1
3	120	10	1.0	97.7	40.7	0.5	38.0
4	130	10	1.0	96.5	65.2	3.0	28.5
5	130	2	3.0	99.7	14.1	0.1	63.5
6	140	2	3.0	98.2	51.6	2.9	25.5
7	150	2	3.0	97.6	37.4	10.6	11.3

Entries 1-4, Beta-30; entries 5-7, Z-5-30

T—Temperature (°C); L—zeolite loading (%, w/w on cellulose); t—hydrolysis time (h); x—cellulose conversion (%); y—glucose yield (%); z—HMF yield (%); and Y—yield of oligosaccharides (%)

two consecutive reactions: cellulose hydrolysis and subsequent glucose degradation, as described below:

$$\text{Cellulose} \xrightarrow{k_1} \text{Glucose} \xrightarrow{k_2} \text{Degradation products} \quad (6)$$
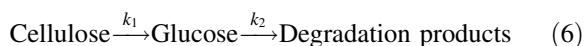
This kinetic model contains two pseudo first-order reactions, and the optimum yield of glucose (y_{opt}, the maximum yield of glucose at certain temperature) could be determined by the value of k_1/k_2. If k_1 increases faster than k_2 with temperature, the value of k_1/k_2 becomes larger, and thus leading to higher y_{opt}. Otherwise, lower y_{opt} is obtained.

As shown in Fig. 5, y_{opt} decreased as temperature increased. That is to say k_2 increased faster than k_1 with reaction temperature. In other words, the glucose degradation to HMF was more sensitive to temperature than the cellulose hydrolysis to glucose. Therefore, it is a better strategy to conduct cellulose hydrolysis at relatively lower temperature (for example, 130 °C) for longer time than at higher temperature for shorter time, in order to improve glucose yield and suppress the formation of HMF.

(3) Zeolite loading

The effect of zeolite loading on the cellulose hydrolysis in LBTH was investigated with the zeolite to cellulose mass ratio between 0.5 and 0.02, and the results are summarized in Table 4. It is clear that the conversion of cellulose readily occurred in the LBTH system at low loading of zeolite as catalyst. For example, almost 100% cellulose could be hydrolyzed
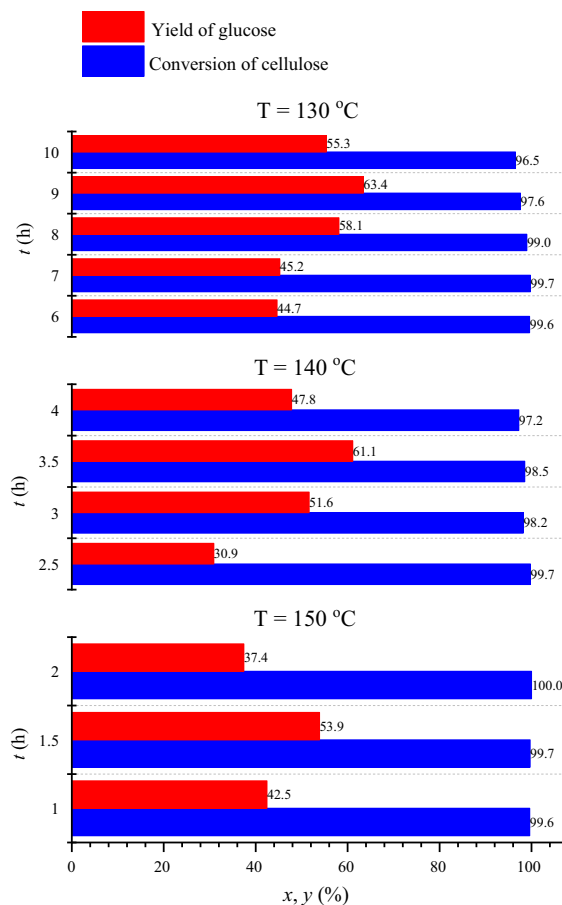

Fig. 5 Cellulose hydrolysis catalyzed by Z-5-30 at different temperature. Hydrolysis condition: zeolites (2%, 0.01 g), Avicel (0.5 g), and 60% w/w LiBr (5 mL). T—temperature (°C); t—hydrolysis time (h); x—cellulose conversion (%); y—glucose yield (%)

with 10% (w/w on cellulose) zeolite at 120 °C (entry 5 and 6). The zeolite loading was much lower than that reported in previous studies (Gonzalez-Rivera et al. 2014; Yu et al. 2018; Zhou et al. 2013). If temperature was elevated to 140 °C, 2% Beta-30 was able to completely hydrolyze cellulose. On the other hand, the yield of glucose was dependent on multiple factors, zeolite loading, reaction time, and temperature. When temperature and time were kept at 120 °C and 30 min, glucose yield linearly increased with zeolite loading (when < 20%), suggesting that the additional solid acid not only ensured the hydrolysis of cellulose to oligosaccharides but also enhanced the hydrolysis of oligosaccharides to glucose. However, excessive Beta-30 (> 20%) could not further improve the glucose yield but promote the dehydration of glucose

Table 4 Results of Beta-30 catalyzed cellulose hydrolysis in LBTH system

Entry	T (°C)	L (%)	t (h)	x (%)	y (%)	z (%)	Y (%)
1	120	100	0.5	96.1	47.3	5.0	38.1
2	120	50	0.5	92.2	60.4	3.7	14.5
3	120	20	0.5	97.6	60.8	1.8	20.3
4	120	15	0.5	96.7	45.6	1.0	41.3
5	120	10	0.5	98.1	28.3	0.2	54.4
6	120	10	1.0	97.7	40.7	0.5	38.0
7	120	5	1.0	69.9	9.3	0.0	47.8
8	140	2	3.5	98.5	61.2	4.7	11.7

T—temperature (°C); L—zeolite loading (%, w/w on cellulose); t—hydrolysis time (h); x—cellulose conversion (%); y—glucose yield (%); z—HMF yield (%); and Y—yield of oligosaccharides (%)

Fig. 6 Cellulose hydrolysis by Beta-30 with different loading at 130 °C. L—zeolite loading (%, w/w on cellulose); t—hydrolysis time (h); x—cellulose conversion (%); y—glucose yield (%); z—HMF yield (%)

to HMF, which was supported by the observation of the low glucose yield (Fig. S3 in ESM) and high HMF yield at extra high zeolite loading. Extending the reaction time at moderate zeolite loading could improve the glucose yield (entry 5 vs. entry 6). Reducing Beta-30 loading from 10% (Entry 6) to 5% (Entry 7), 1-h reaction only hydrolyzed about 70% cellulose and gave 9.3% glucose yield at 120 °C. Increasing temperature could enhance cellulose hydrolysis even at low zeolite loading. For example, cellulose conversion reached 98.5% with a glucose yield of 61.2% at 140 °C with only 2% zeolite loading. However, high temperature promoted the glucose degradation significantly, resulting in a high HMF yield of 4.7%.

To further understand the effect of acid loading, time, and temperature on cellulose hydrolysis, the cellulose hydrolysis was conducted with high zeolite loading (20%) for shorter time (< 3 h) and low zeolite loading (2%) for longer time (> 6 h), respectively, as shown in Fig. 6. It was observed that y_{opt} was higher at high zeolite loading (69.8%) than at low zeolite loading (60.6%), and meanwhile HMF yield was higher at high zeolite loading. The results suggested that cellulose hydrolysis was more sensitive to zeolite loading than glucose degradation. In other words, acid loading was a vital factor to obtain high glucose yield. Overall, the results in Table 4 and Fig. 6 suggested that cellulose hydrolysis should be conducted at moderate temperature, and sufficient hydrolysis time
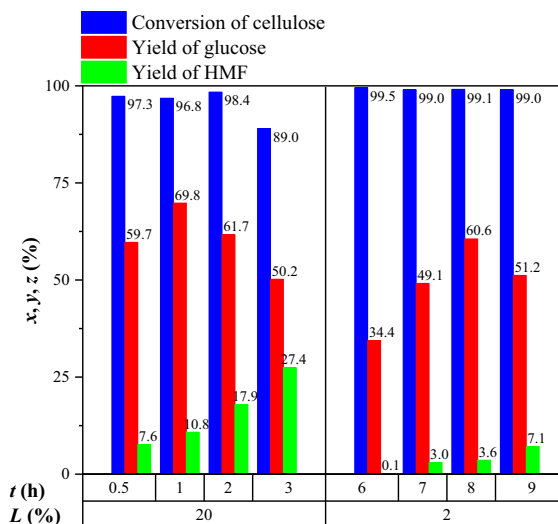
with relatively low but enough solid acid loading to achieve high single pass yield of glucose with limited formation of HMF.

(4)   SiO$_2$/Al$_2$O$_3$ ratio

In many zeolite-catalyzed reactions, acid concentration and acid strength were imperative factors for the yield and selectivity of target product (Chowdhury and Gascon 2018; Kim et al. 2019; Xue et al. 2018). Beta-30 (high H/L ratio) possessed more acid sites than Beta-50 but weaker acid strength because of their different framework aluminum distribution. The acid concentration of Beta-30 was nearly twice that of Beta-50. When Beta-50 loading was twice of Beta-30, they had similar catalytic performance under the same reaction conditions in terms of cellulose hydrolysis, glucose yield, and HMF formation, as shown in Table 5. This observation implied that acid concentration was more important than acid strength, and the distribution of acid sites on framework of zeolite had little influence on cellulose hydrolysis.

Insights into the zeolite-catalyzed cellulose hydrolysis in LBTH system

In our previous studies (Li et al. 2016; Liao et al. 2019), it was observed that the LBTH system has the

Table 5 Comparison of hydrolysis performance of Beta-30 and Beta-50

Entry	Zeolite	T (°C)	t (h)	L (%)	x (%)	y (%)	z (%)	Y (%)
1	Beta-50	120	0.5	100	96.8	59.2	3.4	18.3
2	Beta-50	130	1.5	100	91.9	47.3	6.8	–
3	Beta-30	120	0.5	50	92.2	60.4	3.7	14.7
4	Beta-30	130	1.5	50	97.0	43.2	7.0	–

T—temperature (°C); L—zeolite loading (%, w/w on cellulose); t—hydrolysis time (h); x—cellulose conversion (%); y—glucose yield (%); z—HMF yield (%); and Y—yield of oligosaccharides (%)

ability to solubilize cellulose, and the dissolved cellulose is readily hydrolysable. How cellulose is exactly solubilized in the LBTH system remains unclear, but it is believed that the disruption of the hydrogen bonds between cellulose chains by Li^+ and Br^- is the key step to dissolve cellulose. In the LBTH system, Li^+ is coordinated with water molecules, and Br^- is largely free in the system. The incompletely hydrated lithium cations are able to coordinate with the hydroxyl groups of the cellulose, which would lead to the disruption of the intermolecular hydrogen bond (O(6)H–O(3)) of cellulose. In addition, the coordination of hydrated lithium cations with hydroxyl groups could increase the overall hydrophilicity of cellulose chains and thereby facilitate the dissolution of cellulose. Furthermore, free Br^- in the system would probably promote the dissolution of cellulose by either facilitating the Li–OH coordination or directly interacting with cellulose-OH.

It is known that acidity (activity of proton) of an acid could be enhanced in a molten salt hydrate (Deng et al. 2015; Li et al. 2018a). In other words, the acidity of an acid is higher in molten salt hydrate than in water at the same concentration. To verify whether this is also the case for zeolite in the LBTH, H^+ concentration and pH of Beta-30 in the LBTH were investigated. It is apparent that the pH of 2% Beta-30 in the LBTH was lower than that in water, as shown in Table 6. This was the reason why low zeolite loading was able to efficiently hydrolyze cellulose in the ALBTH. The used Beta-30 had higher pH in the LBTH, suggesting that the H^+ was released via ion-exchange with Li^+ in the system during cellulose hydrolysis. When the used Beta-30 was regenerated, the pH decreased again but did not go back to the level of fresh Beta-30 (Table 6). To verify that H-form zeolite with Brønsted acid sites released H^+ via ion exchange, the acid sites on used

Table 6 Acidity of Beta-30 in LBTH system

Sample	Solvent	pH	γ^a
2% Beta-30	LBTH	3.47	0.89
2% Beta-30	H_2O	5.60	0.01
2% used Beta-30[b]	LBTH	5.20	0.02
2% regenerated Beta-30[b, c]	LBTH	3.93	0.31

[a] pH = $-\lg\gamma[H^+]$. Theoretical $[H^+]$ is calculated based on Py-IR results of fresh Beta-30

[b] Hydrolysis condition: temperature, 130 °C; hydrolysis time, 1 h; loading, 10% w/w on cellulose

[c] Regeneration condition: temperature, 90 °C; time, 3 h; twice

zeolites were investigated by FTIR through pyridine adsorption. As shown in Fig. S4 and Table S3 (in ESM), the used zeolites had almost no Brønsted acid sites, compared to the fresh ones (Table 1). In contrast, the amount of Lewis acid sites decreased only slightly after the hydrolysis. These observations implied that the Brønsted acid sites released H^+ by ion exchange with Li^+ in the LBTH for catalyzing cellulose hydrolysis.

Based on the structural characteristics of the zeolites and the results and observations from the zeolite-catalyzed cellulose hydrolysis tests above, a mechanism of H-form zeolites catalyzing cellulose hydrolysis in the LBTH system could be proposed in Fig. 7. Initially, Li^+ entered the inner channels of H-form zeolite and then ion exchanged with the Brønsted acid sites of H-form zeolite to release H^+ into the solution, which subsequently catalyzed the hydrolysis of dissolved cellulose in the LBTH homogeneously to produce oligosaccharides and glucose. The oligosaccharide was further hydrolyzed into glucose. Part of the glucose could be dehydrated to form HMF under the acid circumstance.
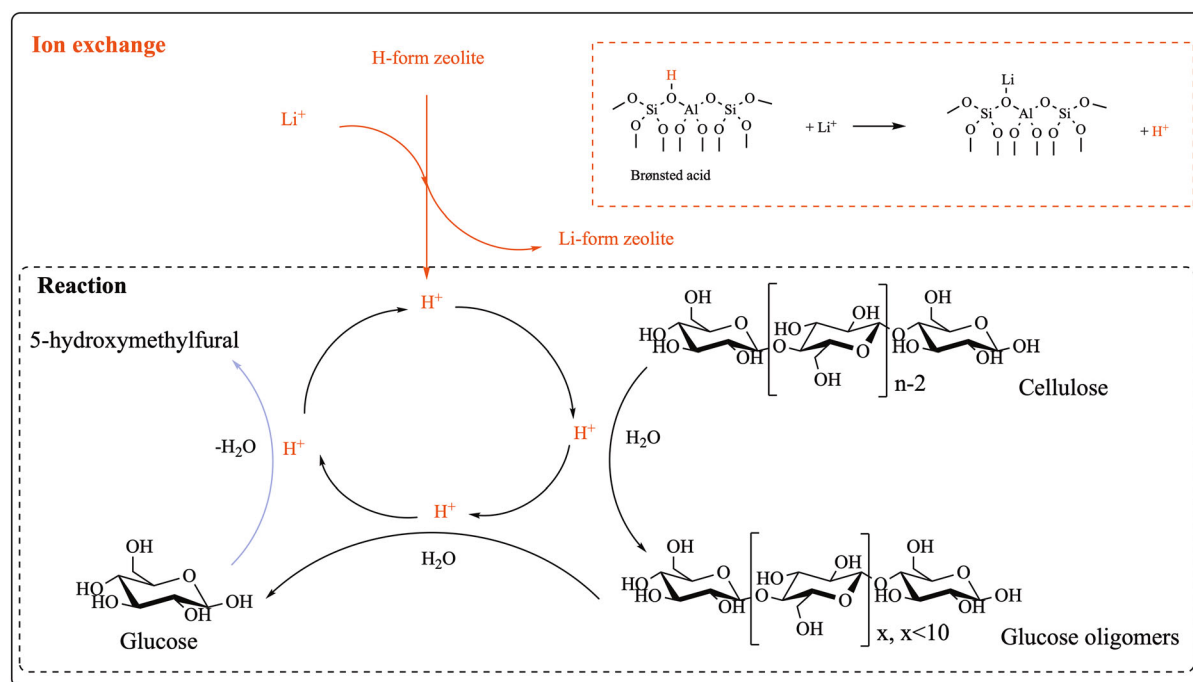
Fig. 7 Proposed reaction pathway of cellulose hydrolysis catalyzed by zeolites in LBTH system

Texture properties (surface area, pore structure, pore volume, and pore size) of zeolites are very important factors in zeolite catalyzed reactions. For example, Fan et al. (Cho et al. 2014) studied zeolite-catalyzed glucose isomerization, and they found that Beta zeolite (5.6–6.7 Å) had better catalytic performance than ZSM-5 (5.1–5.6 Å), because the pores of the latter were too small for glucose to access the active sites located in the inner microporous channels. In the present study, Beta-30 and Z-5-30 exhibited similar performance in catalyzing cellulose hydrolysis in the LBTH system as long as the acid concentration was the same, likely because the reaction mechanism in the LBTH is different from that in water system. Cellulose hydrolysis in water is a typical heterogenous reaction, and cellulose is hydrolyzed only it could access the H-sites of zeolite, which located inside the pores of zeolite catalysts. This is why zeolite is usually not an effective solid acid to catalyze cellulose hydrolysis in water, because cellulose particles are too big to enter the pores and access the acidic sites. However, in the LBTH system, cellulose was dissolved. The cation Li^+ in the solution could easily and quickly access the H-sites in the pore channels of zeolites, ion-exchange with H^+, and release free H^+

into the solution. The H^+ in solution was then able to readily access the dissolved cellulose and catalyze the cleavage of glycosidic bonds of cellulose. In other words, the zeolite-catalyzed cellulose in the LBTH system is a homogeneous reaction in the solution between free H^+ and dissolved cellulose rather than a heterogeneous reaction between solid zeolite and solid cellulose. Therefore, the catalytic activity of the zeolite in the LBTH was independent of the texture properties (such as pore size) but heavily depended on the quantity of acid sites in zeolites.

It was reported that zeolite-catalyzed cellulose hydrolysis in water usually required high temperature or extremely high zeolite loading to obtain a satisfactory glucose yield (Chen et al. 2018; Zhou et al. 2013). However, as observed above, 2% Beta-30 was enough to catalyze cellulose hydrolysis in the LBTH at moderate temperature to a high glucose yield. Another advantage of the LBTH system is the high boiling point (low vapor pressure) of the system, which allows the hydrolysis to be conducted at atmospheric pressure without the need of pressurized reactor.

In summary, the excellent performance of the zeolite in catalyzing cellulose hydrolysis in the LBTH was attributed to the ability of the LBTH system to

dissolve cellulose, the enhanced acidity, and the release of proton from zeolite to solution to hydrolyze the dissolved cellulose. The process of zeolite-catalyzed cellulose hydrolysis in the LBTH can be summarized below. First, cellulose was dissolved in the LBTH to form a homogeneous solution, which made the β-glucosidic bond more readily accessible to the catalyst. Second, proton on the framework of zeolite was exchanged into the solution by Li^+, which could freely reach and hydrolyze cellulose. Third, the activity of the proton was enhanced in the LBTH system, compared to that in an aqueous solution at the same acid concentration, which reduced not only the catalyst loading but also the acid-induced sugar dehydration. Fourth, the dissolved cellulose was hydrolyzed by the free proton homogeneously in the solution.

Recyclability of zeolites

As discussed above, the zeolite hydrolyzed cellulose by releasing H^+ to the solution via ion exchange with Li^+ in the LBTH. After the hydrolysis, the zeolite lost its Brønsted acid sites and thereby catalytic activity. Before the catalyst could be reused, regeneration has to be conducted to restore the acid sites. A common method to convert Na-form zeolite to H-form zeolite in industrial application is to treat the zeolite with ammonium nitrate. The same method was applied to the used Li-form zeolite. The regeneration of Beta-30 under different conditions and the performance of the regenerated Beta-30 are shown in Table 7. For Entry 1, the used zeolite was treated in 1 M NH_4NO_3 solution at 90 °C for 3 h. The regenerated zeolite was

collected by filtration, dried, and calcined at 550 °C for 3 h. The operation was repeated twice. The regenerated Beta-30 was able to hydrolyze (convert) cellulose by ∼ 97%, which was comparable with fresh Beta-30 (Entry 5). However, it seems that the acidity of Beta-30 was not fully recovered, because the glucose and HMF yields were much lower, and oligosaccharide yield was much higher than those by fresh catalyst (Entry 5). Py-FTIR analysis and pH measurement confirmed that only approximately 50% catalytic acidity was recovered (Table S3 in ESM and Table 6). In addition, X-ray fluorescence analysis revealed the difference in elemental composition between fresh and regenerated zeolites. Regenerated zeolite (Entry 1) lost nearly 40% alumina, which serves as Brønsted acid sites. Leaching of framework alumina might be responsible for the loss in catalytic activity and acidity. Milder regeneration conditions (Entries 2–4 in Table 7), such as short time and low temperature, were also tested for the regeneration of Beta-30, but the results were not as good as Entry 1. These observations indicated that the Li-form zeolite was not as hydrothermally stable as Na-form zeolite in ion exchange procedure. It is well known that cations suppress the hydrolysis of Si–O(H)–Al bonds of zeolite in the presence of water at elevated temperatures. Due to larger hydrated radius of Li^+, Li-form zeolite has a lower ion exchange capacity compared with Na-form zeolite, resulting in poor hydrothermal stability (Ji et al. 2019). Further investigation is required to improve the hydrothermal stability of Li-form zeolite.

To investigate the stability of zeolites during the cellulose hydrolysis in the LBTH system, the used

Table 7 Regeneration of Beta-30 for cellulose hydrolysis in the LBTH system

Entry	Regeneration condition				Hydrolysis performance[a]			
	T (°C)	Reagent	Time (h)	Times	x (%)	y (%)	z (%)	Y (%)
1	90	NH_4NO_3	3.0	Twice	96.7	27.4	0.2	60.3
2	90	NH_4NO_3	3.0	Once	70.1	15.2	0.1	47.1
3	90	NH_4NO_3	1.0	Once	65.7	10.3	0.1	43.6
4	50	NH_4NO_3	3.0	Twice	91.3	20.9	0.2	62.2
5	–	–	–	–	96.5	65.2	3.0	28.5

T—regeneration temperature (°C); x—cellulose conversion (%); y—glucose yield (%); z—HMF yield (%); and Y—yield of oligosaccharides (%)

[a]Hydrolysis condition: temperature, 130 °C; hydrolysis time, 1 h; loading, 10% w/w on cellulose

zeolites from cellulose hydrolysis were recovered, regenerated by the method for Entry 1 in Table 7, and reused for cellulose hydrolysis for ten times. As shown in Fig. 8, zeolites (both Beta-30 and Z-5-30) lost their catalytic activity sharply after the first run of cellulose hydrolysis. Interestingly, cellulose conversion only declined slightly, but the glucose yield dropped sharply, suggesting that the acidity of the regenerated zeolites was still sufficient to hydrolyze cellulose to oligosaccharides but not strong enough to further hydrolyze the oligosaccharides to glucose. This was apparently attributed to the loss of acid sites of the zeolites due to the incomplete transformation of Li-form to H-form during the regeneration and the loss of unstable framework alumina, as discussed above. However, from the second run of the hydrolysis, the catalytic capacity of the zeolites became relatively stable, and the glucose yield decreased slowly. For example, Beta-30 achieved 55.8% glucose yield in the first run, which dropped to 27.4% in the second run, but still maintained 22.6% in the tenth run. These observations suggested that after the dealumination due to the removal of unstable framework alumina, the zeolites became hydrothermally more stable, and thereby their catalytic activity kept relatively stable. On the other hand, to achieve the same glucose yield as fresh zeolites, the loading of regenerated zeolites should be higher to complement the lost acidity.
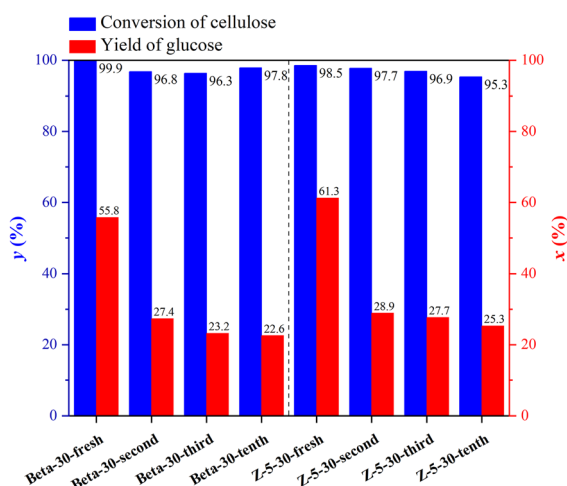

Fig. 8 Recyclability and stability of zeolites. Hydrolysis condition: zeolite, 0.05 g; Avicel, 0.5 g; 60% w/w LiBr, 5.00 mL; 1 h and 130 °C. x—cellulose conversion (%); y—glucose yield (%)

Conclusion

Two types of zeolites (Beta and ZSM-5) were synthesized and demonstrated as solid acid catalysts for cellulose hydrolysis in inorganic ionic liquid (the LBTH) system at moderate temperature without a pretreatment process. In the LBTH system, cellulose was dissolved, and the ion exchange between Li^+ and the H-sites of zeolite released H^+ into the solution, which achieved homogeneous cellulose hydrolysis. As a result, cellulose could be completely hydrolyzed with only 2% zeolite at 140 °C within 3.5 h with a single-pass glucose yield > 60%. The catalytic activity of fresh zeolite could be recovered about 50% by regeneration after the first run, and the catalytic activity of used zeolite kept stable in the following runs.

Authors' contribution XP initiated this study. All authors contributed to the study conception and design. Material preparation, data collection, and analysis were performed by TW and XP. The first draft of the manuscript was prepared by TW, and all authors commented and revised the manuscript. All authors read and approved the final manuscript.

Compliance with ethical standards

Conflict of interest The authors declare that they have no conflict of interest.

References

Cai H, Li C, Wang A, Xu G, Zhang T (2012) Zeolite-promoted hydrolysis of cellulose in ionic liquid, insight into the mutual behavior of zeolite, cellulose and ionic liquid. Appl Catal B 123–124:333–338. https://doi.org/10.1016/j.apcatb.2012.04.041

Chen TL, Xiong CR, Tao YS (2018) Enhanced hydrolysis of cellulose in ionic liquid using mesoporous ZSM-5. Molecules 23:1–10. https://doi.org/10.3390/molecules23030529

Cho HJ, Dornath P, Fan W (2014) Synthesis of hierarchical Sn-MFI as Lewis acid catalysts for isomerization of cellulosic sugars. ACS Catal 4:2029–2037. https://doi.org/10.1021/cs500295u

Chowdhury AD, Gascon J (2018) The curious case of ketene in zeolite chemistry and catalysis. Angew Chemie-Int Edn 57:14982–14985. https://doi.org/10.1002/anie.201808480

Chu S, Ln Yang, Guo X, Dong L, Chen X, Li Y, Mu X (2018) The influence of pore structure and Si/Al ratio of HZSM-5

zeolites on the product distributions of α-cellulose hydrolysis. Mol Catal 445:240–247. https://doi.org/10.1016/j.mcat.2017.11.032

Deng W, Kennedy JR, Tsilomelekis G, Zheng W, Nikolakis V (2015) Cellulose hydrolysis in acidified LiBr molten salt hydrate media. Ind Eng Chem Res 54:5226–5236. https://doi.org/10.1021/acs.iecr.5b00757

Etim UJ, Bai P, Wang Y, Subhan F, Liu Y, Yan Z (2019) Mechanistic insights into structural and surface variations in Y-type zeolites upon interaction with binders. Appl Catal A 571:137–149. https://doi.org/10.1016/j.apcata.2018.12.013

Ferreira Madeira F, Ben Tayeb K, Pinard L, Vezin H, Maury S, Cadran N (2012) Ethanol transformation into hydrocarbons on ZSM-5 zeolites: influence of Si/Al ratio on catalytic performances and deactivation rate. Study of the radical species role. Appl Catal A 443–444:171–180. https://doi.org/10.1016/j.apcata.2012.07.037

Franzyshen SK, Schiavelli MD, Stocker KD, Ingram MD (1990) Proton acidity and chemical reactivity in molten salt hydrates. J Phys Chem 94:2684–2688. https://doi.org/10.1021/j100369a082

Gonzalez-Rivera J, Galindo-Esquivel IR, Onor M, Bramanti E, Longo I, Ferrari C (2014) Heterogeneous catalytic reaction of microcrystalline cellulose in hydrothermal microwave-assisted decomposition: effect of modified zeolite Beta. Green Chem 16:1417–1425. https://doi.org/10.1039/c3gc42207k

Guo Y, Sun T, Liu X, Ke Q, Wei X, Gu Y, Wang S (2019) Cost-effective synthesis of CHA zeolites with controllable morphology and size. Chem Eng J 358:331–339. https://doi.org/10.1016/j.cej.2018.10.007

Hammerer F, Loots L, Do JL, Therien JPD, Nickels CW, Friscic T, Auclair K (2018) Solvent-free enzyme activity: quick, high-yielding mechanoenzymatic hydrolysis of cellulose into glucose. Angew Chemie-Int Edn 57:2621–2624. https://doi.org/10.1002/anie.201711643

Huang Y-B, Fu Y (2013) Hydrolysis of cellulose to glucose by solid acid catalysts. Green Chem 15:1095–1111. https://doi.org/10.1039/C3GC40136G

Huang L et al (2019) Enhanced hydrolysis of cellulose by catalytic polyethersulfone membranes with straight-through catalytic channels. Biores Technol 294:122119. https://doi.org/10.1016/j.biortech.2019.122119

Ji Y, Yang H, Yan W (2019) Effect of alkali metal cations modification on the acid/basic properties and catalytic activity of ZSM-5 in cracking of supercritical n-dodecane. Fuel 243:155–161. https://doi.org/10.1016/j.fuel.2019.01.105

Jiang C-W, Zhong X, Luo Z-H (2014) An improved kinetic model for cellulose hydrolysis to 5-hydroxymethylfurfural using the solid SO_4^{2-}/Ti-MCM-41 catalyst. RSC Adv 4:15216–15224. https://doi.org/10.1039/C4RA00167B

Jiang L-q, Zheng A-q, Meng J-g, Wang X-b, Zhao Z-l, Li H-b (2019) A comparative investigation of fast pyrolysis with enzymatic hydrolysis for fermentable sugars production from cellulose. Biores Technol 274:281–286. https://doi.org/10.1016/j.biortech.2018.11.098

Kim KD, Wang Z, Jiang Y, Hunger M, Huang J (2019) The cooperative effect of Lewis and Brønsted acid sites on Sn-MCM-41 catalysts for the conversion of 1,3-dihydroxyacetone to ethyl lactate. Green Chem 21:3383–3393. https://doi.org/10.1039/C9GC00820A

Li N, Pan X, Alexander J (2016) A facile and fast method for quantitating lignin in lignocellulosic biomass using acidic lithium bromide trihydrate (ALBTH). Green Chem 18:5367–5376. https://doi.org/10.1039/C6GC01090C

Li N, Li Y, Yoo CG, Yang X, Lin X, Ralph J, Pan X (2018a) An uncondensed lignin depolymerized in the solid state and isolated from lignocellulosic biomass: a mechanistic study. Green Chem 20:4224–4235. https://doi.org/10.1039/C8GC00953H

Li X, Peng K, Xia Q, Liu X, Wang Y (2018b) Efficient conversion of cellulose into 5-hydroxymethylfurfural over niobia/carbon composites. Chem Eng J 332:528–536. https://doi.org/10.1016/j.cej.2017.06.105

Liao Y, Pang Z, Pan X (2019) Fabrication and mechanistic study of aerogels directly from whole biomass. ACS Sustain Chem Eng 7:17723–17736. https://doi.org/10.1021/acssuschemeng.9b04032

Marianou AA, Michailof CM, Pineda A, Iliopoulou EF, Triantafyllidis KS, Lappas AA (2018) Effect of Lewis and Brønsted acidity on glucose conversion to 5-HMF and lactic acid in aqueous and organic media. Appl Catal A 555:75–87. https://doi.org/10.1016/j.apcata.2018.01.029

Mu B, Xu H, Li W, Yang Y (2019) Quantitation of fast hydrolysis of cellulose catalyzed by its substituents for potential biomass conversion. Biores Technol 273:305–312. https://doi.org/10.1016/j.biortech.2018.11.039

Onda A, Ochi T, Yanagisawa K (2008) Selective hydrolysis of cellulose into glucose over solid acid catalysts. Green Chem 10:1033–1037. https://doi.org/10.1039/B808471H

Rinaldi R, Schuth F (2010) Acid hydrolysis of cellulose as the entry point into biorefinery schemes. Chemsuschem 3:296. https://doi.org/10.1002/cssc.201090010

Saeman JF (1945) Kinetics of wood saccharification - hydrolysis of cellulose and decomposition of sugars in dilute acid at high temperature. Ind Eng Chem 37:43–52. https://doi.org/10.1021/ie50421a009

Shrotri A, Kobayashi H, Fukuoka A (2018) Cellulose depolymerization over heterogeneous catalysts. Acc Chem Res 51:761–768. https://doi.org/10.1021/acs.accounts.7b00614

Shuai L, Yang Q, Zhu JY, Lu FC, Weimer PJ, Ralph J, Pan XJ (2010) Comparative study of SPORL and dilute-acid pretreatments of spruce for cellulosic ethanol production. Biores Technol 101:3106–3114. https://doi.org/10.1016/j.biortech.2009.12.044

Swift TD, Nguyen H, Erdman Z, Kruger JS, Nikolakis V, Vlachos DG (2016) Tandem Lewis acid/Brønsted acid-catalyzed conversion of carbohydrates to 5-hydroxymethylfurfural using zeolite beta. J Catal 333:149–161. https://doi.org/10.1016/j.jcat.2015.10.009

Woolery GL, Kuehl GH, Timken HC, Chester AW, Vartuli JC (1997) On the nature of framework Brønsted and Lewis acid sites in ZSM-5. Zeolites 19:288–296. https://doi.org/10.1016/S0144-2449(97)00086-9

Wu T, Yuan G, Chen S, Xue Y, Li S (2017) Synthesis of ZSM-5 and its application in butylene catalytic cracking. J Fuel Chem Technol 45:182–188. https://doi.org/10.1016/S1872-5813(17)30013-0

Wu T, Yuan G, Chen S-L, Zhao D, Xu J, Fan T, Cao Y (2018) Butylene catalytic cracking to propylene over a hierarchical HZSM-5 zeolite: location of acid sites controlling the reaction pathway. Mol Catal 453:161–169. https://doi.org/10.1016/j.mcat.2018.04.026

Xiang M, Wu D (2019) Facile preparation of pore- and morphology-controllable ETS-10 zeolite with enhanced biomass hydrogenation activity. Chem Eng J 369:180–194. https://doi.org/10.1016/j.cej.2019.03.058

Xue N et al (2018) Hydrolysis of zeolite framework aluminum and its impact on acid catalyzed alkane reactions. J Catal 365:359–366. https://doi.org/10.1016/j.jcat.2018.07.015

Yang XH, Li N, Lin XL, Pan XJ, Zhou YH (2016) Selective cleavage of the aryl ether bonds in lignin for depolymerization by acidic lithium bromide molten salt hydrate under mild conditions. J Agric Food Chem 64:8379–8387. https://doi.org/10.1021/acs.jafc.6b03807

Yu J, Wang J, Wang Z, Zhou M, Wang H (2018) Catalytic performance of silicalite-1 modified HY zeolite in the hydrolysis of cellulose. J Fuel Chem Technol 46:1447–1453. https://doi.org/10.1016/S1872-5813(18)30058-6

Zhang Z, Zhao ZK (2009) Solid acid and microwave-assisted hydrolysis of cellulose in ionic liquid. Carbohyd Res 344:2069–2072. https://doi.org/10.1016/j.carres.2009.07.011

Zhou L, Liu Z, Shi M, Du S, Su Y, Yang X, Xu J (2013) Sulfonated hierarchical H-USY zeolite for efficient hydrolysis of hemicellulose/cellulose. Carbohyd Polym 98:146–151. https://doi.org/10.1016/j.carbpol.2013.05.074